



This is a repository copy of *Winding configurations and performance of heteropolar electrodynamic magnetic bearings*.

White Rose Research Online URL for this paper:

<https://eprints.whiterose.ac.uk/id/eprint/232576/>

Version: Published Version

Article:

Alzhrani, A. and Atallah, K. orcid.org/0000-0002-8008-8457 (2025) Winding configurations and performance of heteropolar electrodynamic magnetic bearings. IET Electric Power Applications, 19 (1). e70105. ISSN: 1751-8660

<https://doi.org/10.1049/elp2.70105>

Reuse

This article is distributed under the terms of the Creative Commons Attribution (CC BY) licence. This licence allows you to distribute, remix, tweak, and build upon the work, even commercially, as long as you credit the authors for the original work. More information and the full terms of the licence here:

<https://creativecommons.org/licenses/>

Takedown


If you consider content in White Rose Research Online to be in breach of UK law, please notify us by emailing eprints@whiterose.ac.uk including the URL of the record and the reason for the withdrawal request.



eprints@whiterose.ac.uk
<https://eprints.whiterose.ac.uk/>

ORIGINAL RESEARCH OPEN ACCESS

Winding Configurations and Performance of Heteropolar Electrodynamic Magnetic Bearings

Abdoalateef Alzhrani¹ | Kais Atallah² 
¹Department of Electrical Engineering, JIC, Royal Commission for Jubail and Yanbu, Al Jubail, Saudi Arabia | ²School of Electrical and Electronic Engineering, University of Sheffield, Sheffield, UK

Correspondence: Kais Atallah (k.atallah@sheffield.ac.uk)

Received: 3 March 2025 | **Revised:** 10 September 2025 | **Accepted:** 19 September 2025

Handling Editor: Mihai Comanescu

Funding: The authors received no specific funding for this work.

Keywords: magnetic bearings | magnetic levitation | permanent magnets

ABSTRACT

The requirement for high speed reliable and efficient bearing operation drove the research into magnetic bearings. In the past decades, active magnetic bearings (AMBs), which are known for their operational cost and complexity, have received significant attention, and have been utilised in high-speed industrial applications. On the other hand, electrodynamic magnetic bearings (EDBs) are a different type of magnetic bearing that offers passive, efficient and more importantly stable operation. Nevertheless, despite these advantages, EDBs have received relatively little attention. This paper focuses on the heteropolar variant of EDB, with particular emphasis on winding configurations and the effects of design parameters. A comparison between winding configurations recommended in the literature and a simpler winding configuration proposed by the authors is undertaken. It is shown that both winding configurations exhibit similar performance, in terms of restoring force production and stability. Furthermore, the effects of the leading design parameters of EDB employing the proposed windings are investigated. Moreover, to validate some of the findings a test rig is developed, and good agreement between measured and predicted forces is shown for different eccentricities.

1 | Introduction

The rise of high rotational speed applications in various industrial sectors, such as energy storage and generation, space and medical, underpins the requirement for more efficient and reliable bearings [1]. Thus, mechanical bearings became less attractive in such applications due to their inherent shortcomings, such as high losses and reduced lifetime at high speed [2]. Therefore, magnetic levitation emerges as an alternative solution to provide bearing operation for high-speed applications, due to their ability to perform well in severe environments and the absence of lubrication [3]. AMBs are the first to be investigated and utilised in industry. They exhibit larger restoring forces and stable operation over wider speed ranges [4]. Yet,

they are relatively complex, requiring control electronics and associated sensing [5], where in some applications requiring high reliability and limited accessibility, passive alternatives may be preferred. On the other hand, passive magnetic bearings (PMBs) can enable rotor levitation without the requirement for control electronics and sensors. PMBs employ permanent magnets (PMs) to provide magnetic fields and eliminate the need for external excitation. Based on magnetic field configuration and/or principle of the restoring force generation, different PMB topologies exist [6–13]. Some of those types, such as those using PMs and rotating and stationary parts, are used in applications such as energy storage flywheels [14–16] despite their inherent instability as per Earnshaw's theorem [17], albeit in combination with mechanical counterparts.

This is an open access article under the terms of the [Creative Commons Attribution](https://creativecommons.org/licenses/by/4.0/) License, which permits use, distribution and reproduction in any medium, provided the original work is properly cited.

© 2025 The Author(s). *IET Electric Power Applications* published by John Wiley & Sons Ltd on behalf of The Institution of Engineering and Technology.

The need for stability at high speed lead to research into EDBs, which is another type of PMB [18]. EDBs can be configured to control the radial and/or axial degrees of freedom, where restoring force arises as a result of conducting element exposure to magnetic field variation. Compared to other types of PMBs, EDBs offer stable operation at high rotational speed and potential ease of manufacturing. Depending on the spatial variation of the magnetic field, two types of EDB exist: namely, heteropolar EDBs and homopolar EDBs, Figure 1.

Although EDBs offer advantages, in terms of being passive and stable, compared to other magnetic bearings, some factors limited their development. Proposed homopolar topologies, exhibit low stiffness, and poor stability at low rotational speeds [18–20], in addition to the relatively limited understanding of the effects of their design parameters. Albeit, homopolar topologies with significantly improved stiffness have recently been proposed [21]. Furthermore, for the heteropolar topologies considered in the paper, and to the authors' knowledge there has been limited studies which encompasses in-depth analysis of the effects of leading design parameters and some form of experimental validation.

In this paper, the winding configurations in radial field heteropolar EDBs consisting of a rotating multiple PM array interacting with a short-circuited static winding are discussed and the performance of a heteropolar EDB employing a proposed winding configuration is presented. The effects of leading design parameters on stability and stiffness are investigated, and predictions are validated on the prototype EDB.

The structure of the paper is as follows:

- Section 2 discusses the winding configurations under consideration, including the principle of operation, finite element modelling, and performance.
- Section 3 examines the influence of key design parameters, such as conductor shape, number of PM pole pairs, PM thickness, number of coils, and fill factor.
- Section 4 presents the experimental validation, in which a purpose-built test rig is developed to accurately impose eccentricity and measure restoring forces under quasi-static operating conditions.
- Section 5 summarises the main findings.

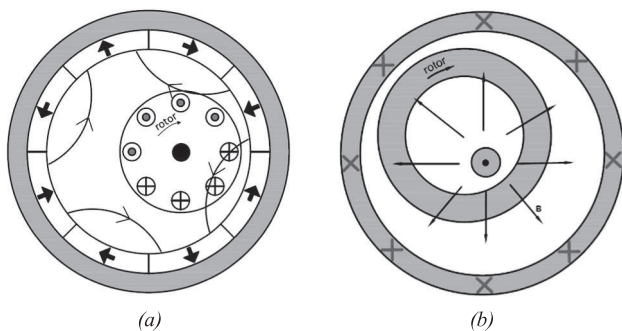


FIGURE 1 | Example of electrodynamic radial bearings showing a heteropolar configuration in (a) and homopolar configuration in (b).

2 | Winding Configurations

2.1 | Principle of Operation

The EDBs presented in this paper are aimed at the control of the degree of freedom perpendicular to the axis of rotation. Hence, the magnitude of restoring force in the axis parallel to eccentricity is one of the main performance indicators. Another factor in assessing the EDBs' performance is the stability threshold speed, which represents the speed beyond which the EDB becomes stable [18]. Heteropolar EDBs consist of a rotating P_m pole-pair PM array and a stator equipped with a short-circuited winding mounted on a nonmagnetic core, as per Figure 2. When the rotor is concentric with the stator, there is no flux linking the coils, and no EMF is induced. Therefore, currents and restoring forces are only present when eccentricity exists. Different winding arrangements are proposed in refs. [22–24], but with limited analysis and performance comparison.

The winding arrangement of the EDB is key to achieving the desired bearing characteristic, that is, null linkage flux, no induced electromotive forces in the absence of rotor eccentricity, and a large restoring force parallel to the direction of eccentricity. A general concept of heteropolar EDB's winding was introduced in ref. [2]. In ref. [23], the conditions for achieving null flux in the absence of eccentricity and restoring force production with eccentricity are introduced. For the null flux linkage condition, the following relationship must hold:

$$mP_s \neq nP_m \quad (1)$$

For any combination (m, n) , where m and n are space harmonics in the magnetic fields produced by the stationary P_s pole-pair winding and the P_m pole-pair PM array, respectively. For force production under eccentricity, the following is proposed:

$$mP_s = nP_m \pm 1 \quad (2)$$

For at least one combination (m, n) . Therefore, it was recommended, as a design guideline, that the number of pole-pairs of the stator winding and the PM array should preferably satisfy:

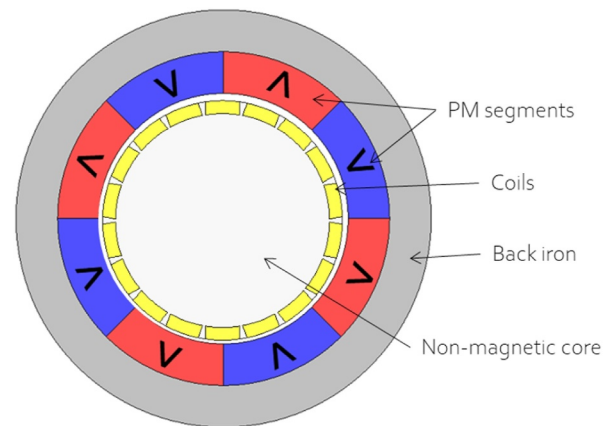


FIGURE 2 | Cross-sectional view of the multi-phase heteropolar EDB.

$$P_s = P_m \pm 1 \quad (3)$$

On the basis that the fundamental components of the winding and the PM array $m = 1$ and $n = 1$, respectively, interact to produce the restoring force.

However, a 2-pole, $P_s = 1$, multiphase winding, comprising a set of circumferentially evenly spaced, fully pitched, and short-circuited coils, can achieve comparable performance. Through the interaction of the PM array fundamental component, $n = 1$ and a higher-order winding space harmonic, $m = 3; 5; 7; \dots$, for $p_m = 4; 6; 8; \dots$, respectively.

A three-phase winding configuration that satisfies Equation (3) is shown in Figure 3. Figure 4, on the other hand, shows the winding configuration for the proposed winding arrangement where $P_m = 4$ and $P_s = 1$, consisting of 9 sets of equispaced, fully-pitched, short-circuited coils.

2.2 | Finite Element Modelling

The required heteropolar EDB geometry was modelled in 2D finite element analysis. Unlike homopolar EDBs, where 3D analyses are required due to the nature of the magnetic field distribution, EDBs with heteropolar magnetic fields can be analysed in 2D, albeit a 3D analysis would also be required for examples with very short axial length. In order to fairly compare the bearing performance of the three-phase winding configuration recommended in [23] and the multi-phase winding configuration, some design parameters must be fixed. The outer

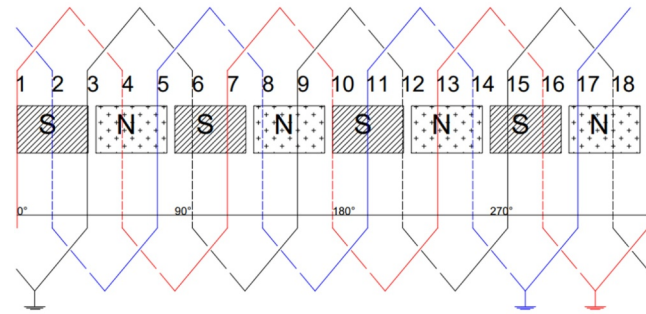


FIGURE 3 | The winding configuration for a topology with ($P_m = 4, P_s = 3$) showing all three phases.

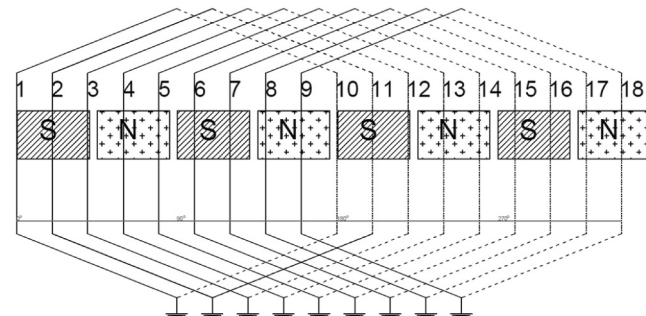


FIGURE 4 | Full winding configuration for topology with ($P_m = 4, P_s = 1$), fully-pitched, and 9 short-circuited coils.

diameters, axial lengths, volume of conductors, and PMs are the same. The common design parameters are detailed in Table 1. Table 2 shows the properties of the assigned material for each part.

2.3 | Bearing Performance

This section presents the bearing performance of the three-phase winding configuration in Figure 3 and the multi-phase winding configuration, shown in Figure 4. The variation of restoring force developed with rotational speed, Joule losses, and stability are presented. The winding configuration of the two considered bearings shares the same number of slots. However, the multiphase winding configuration consists of 9 fully-pitched, short-circuited coils, as shown in Figure 4.

Figure 5 shows the variation of the EDB restoring force with speed for the two winding arrangements. Namely, the three-

TABLE 1 | Parameters common to both EDBs.

Eccentricity	0.1 mm
Air-gap length	1 mm
Rotational speed	1–60krpm
Outer diameter	50 mm
Axial length	100 mm
PM thickness	5 mm
Back iron thickness	5 mm
PM pole-pair number	4

TABLE 2 | Material selection for the heteropolar EDBs.

PM	NdFeB (Br = 1.4 T)
Back-iron	Mild steel
Conductor material	Copper

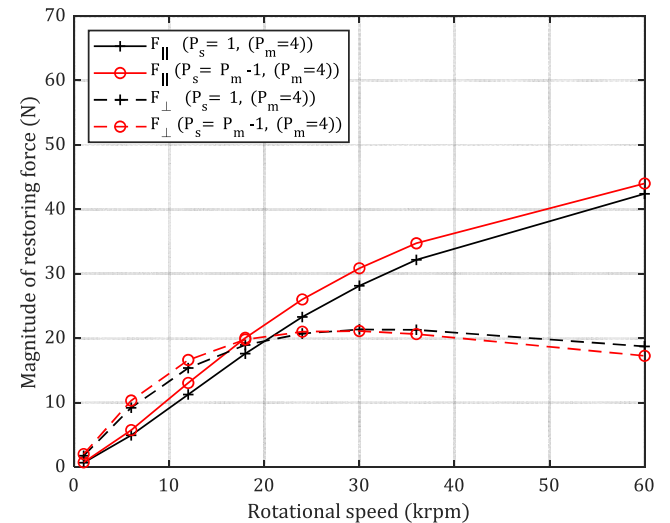


FIGURE 5 | Variation of restoring forces with rotational speed.

phase winding ($P_m = 4, P_s = 3$) and the multi-phase winding ($P_m = 4, P_s = 1$). It can be seen that at lower speeds, the restoring force perpendicular to the direction of eccentricity is higher than the force parallel to eccentricity. However, at 60,000 rpm, the bearings are able to achieve a restoring force of in excess of 40N parallel to the direction of eccentricity, with the perpendicular force being less than 20N.

Because the restoring force in the perpendicular axis is higher than the force in the parallel axis at lower speeds, it was only possible to achieve stability at speeds higher than 20,000 rpm. This can be seen in Figure 6, which shows the variation of the ratio of perpendicular force to the parallel force with speed. Of course, generating high restoring force requires higher current flow in the coils, which results in higher losses. As can be seen in Figure 7, which shows the variation of losses with speed.

From the presented results, both multi-phase winding and three-phase winding configurations achieve similar bearing

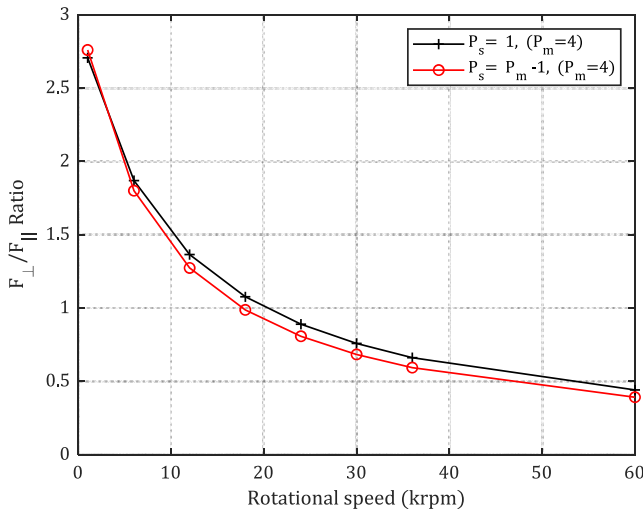


FIGURE 6 | Variation of the ratio of perpendicular force to parallel force with speed.

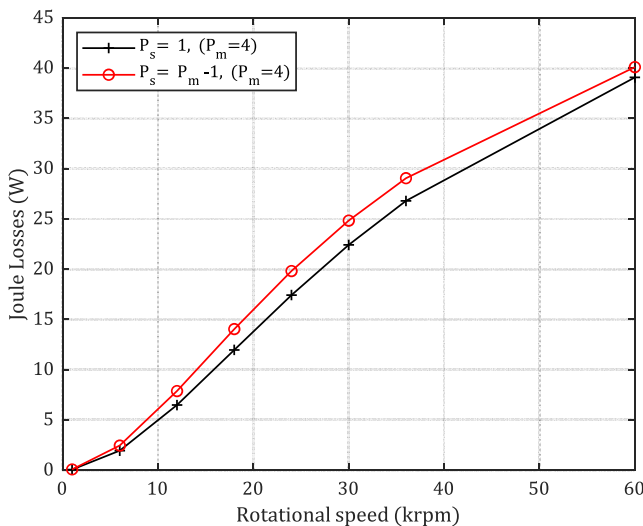


FIGURE 7 | Variation of Joule losses with rotor speed.

performance. However, the advantage of a multi-phase configuration is simplicity and ease of manufacturing, which, hence, potentially reduces costs.

3 | Effect of Leading Design Parameters

This section aims to explore the effects of the leading design parameters, such as conductor shape, PM thickness, and number of PM poles and coils, on the performance of heteropolar EDBs equipped with multi-phase winding with $P_s = 1$.

3.1 | Effect of Conductor Shape

In order to examine the effect of the conductor's shape, in terms of the ratio of the radial thickness to circumferential thickness, an EDB equipped with a fully pitched, single short-circuited coil was chosen for simplicity, Figure 8. In the analysis, the coil span is 180° mechanical, and the cross-sectional area of the conductor is kept constant at $\sim 13.6 \text{ mm}^2$. The main goal of this is to determine the best combination of conductor radial and circumferential thickness, resulting in the highest magnitude of force at a given eccentricity.

The average restoring force over one complete mechanical cycle was considered in this study, and the result is taken by averaging the results of the restoring force over a complete mechanical cycle. Figure 9 shows the variation of the average restoring force in the direction of eccentricity with the ratio of the radial to circumferential thicknesses of the conductor at a rotational speed of 60,000 rpm. It can be seen that there is an optimum ratio that maximises force.

3.2 | Effect of the Number of PM Pole-Pairs

This study aims to understand and evaluate the effect of pole-pair numbers on the performance of heteropolar EDBs equipped with multi-phase winding. This includes the restoring force, stability as well as Joule losses. Furthermore, while changing the pole-pair number, the volume of the PM is kept constant. The parameters of the EDB under investigation are detailed in Table 3.

Figure 10 shows the variation of the restoring force with the number of pole-pairs at different speeds. It can be seen that the

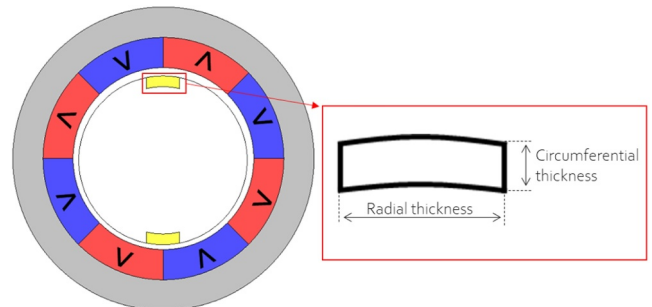


FIGURE 8 | Heteropolar EDB with a single coil.

highest restoring forces occur for pole-pairs between 4 and 6. Therefore, EDB topology with 4, 5, and 6 pole-pair numbers offers the best performance in terms of restoring force magnitude.

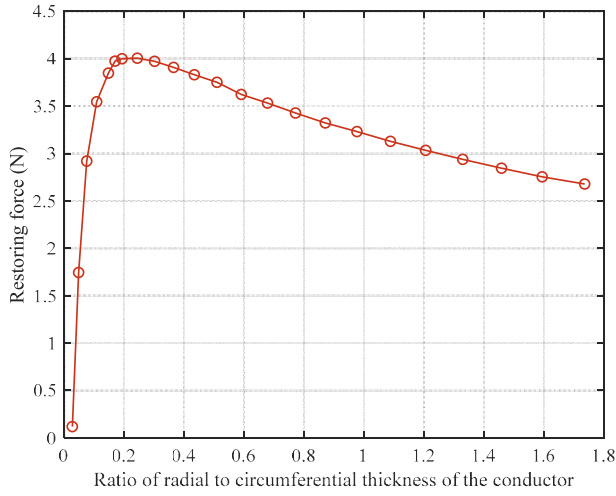


FIGURE 9 | Variation of restoring forces with conductor width ratio (single coil).

TABLE 3 | Parameters of EDBs with different PM pole-pairs.

Winding type	Multi-phase
Eccentricity	0.1 mm
Air-gap length	1 mm
Rotational speed	1–60 krpm
Outer diameter	50 mm
Axial length	100 mm
PM thickness	5 mm
Back iron thickness	5 mm
Number coils	9
PM pole-pair number	2, 4, 6, 8, 10

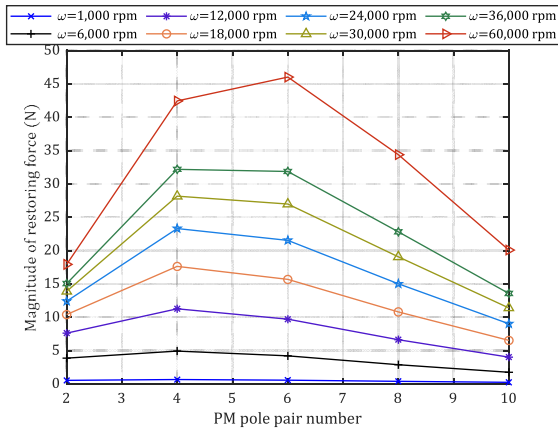


FIGURE 10 | Variation of restoring forces with PM pole-pair number at different rotational speeds.

Figure 11 shows the variation of the ratio of perpendicular force to parallel force, where it can be seen that the ratio remains fairly constant when the number of pole-pairs is larger than 4. Figure 12 shows the variation of the losses with pole-pair numbers at different speeds. It can be noticed that six pole-pairs topology produces 100% more losses compared to four pole-pair, with almost the same amount of restoring force acquired in both topologies.

3.3 | Effect of PM Thickness

This study aims to understand the impact of PM thickness on the bearing performance. For the same winding configuration of $P_m = 4, P_s = 1$, the PM thickness is varied between 1 and 10 mm and the bearing forces, stability ratio as well as Joule losses induced were recorded. Multi-phase winding configuration with nine shorted coils is utilised to conduct this study. Table 4 shows the full design parameters.

Figure 13 shows the variation of the restoring force with PM thickness at different rotational speeds. The effect of increasing the magnet thickness is notable, where an increase in the force is seen as the PM thickness increases. However, the increase in the generated force at lower PM thickness is greater than the

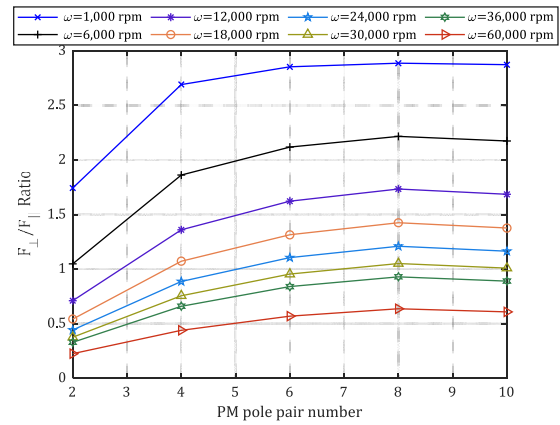


FIGURE 11 | Variation of the ratio of perpendicular force to parallel force with PM pole-pair number.

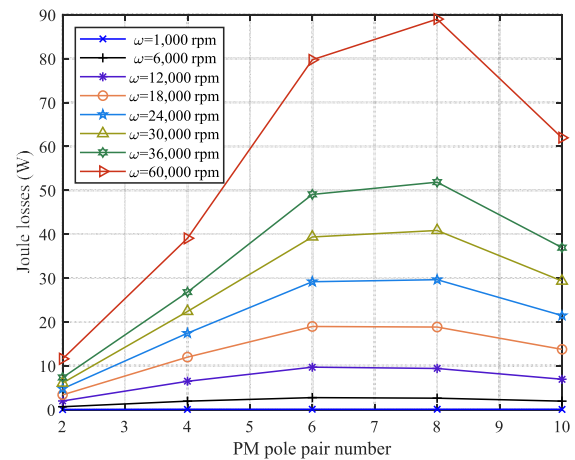


FIGURE 12 | Variation of Joule losses with PM pole-pair number.

increase in the force at higher PM thicknesses. Nevertheless, PM thickness doesn't have a significant effect on stability, as can be seen in Figure 14. Figure 15 shows the variation of the losses with the PM thickness, where it shows a similar trend to that of the forces exists. Indeed, the increase in the losses is more pronounced at higher PM thicknesses.

TABLE 4 | Parameters of EDBs with different PM thicknesses.

Winding type	Mutli-phase
Eccentricity	0.1 mm
Air-gap length	1 mm
Rotational speed	1–60 krpm
Air-gap diameter	30 mm
Axial length	100 mm
PM thickness	1–10 mm
Back iron thickness	5 mm
Number of coils	9
PM pole-pair number	4

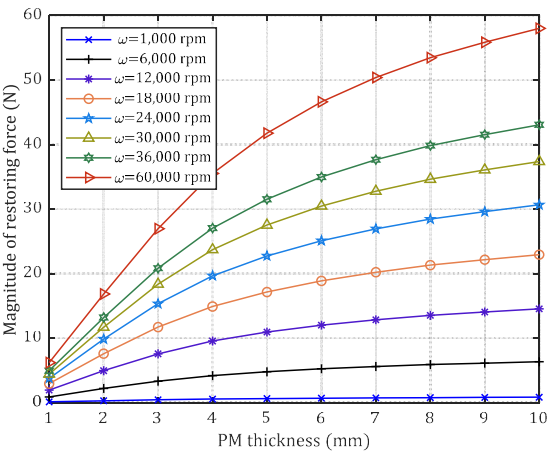


FIGURE 13 | Variation of restoring forces with PM thickness at different rotational speed.

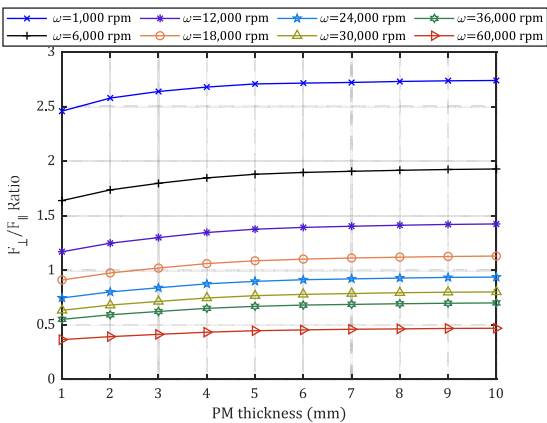


FIGURE 14 | Variation of the ratio of perpendicular force to parallel force with PM thickness.

3.4 | Effect of the Number of Coils

This section focuses on the effect of the number of coils on the bearing performance. In order to understand how the number of shorted coils affects the bearing stiffness, stability, and Joule losses. In the analysis, the copper's volume and the fill factor are kept constant. The fixed design parameters are shown in Table 5.

Figure 16 shows the variation of the bearing forces with the number of coils. It can be seen that for a given speed, the restoring force magnitude tends to increase as the number of coils increases. However, the increase becomes less pronounced beyond a certain number of coils. For example, at 60,000 rpm, the force generated using 9 coils is approximately 100% more than at 3 coils. Yet, it only increases by 7% when 19 coils are used compared to 9 coils. Therefore, the number of coils has a significant effect on the magnitude of the restoring force, even though it does not have a great impact on stability, as shown in Figure 17. Furthermore, losses will also increase when the number of coils is increased, as can be seen in Figure 18, which shows the variation of the losses with the number of coils at different speeds. Albeit, the rate of increase is significantly reduced, beyond 4–5 coils. Normally, the selection of the number of coils will depend on the restoring force and the manufacturing complexity. For example, for this particular

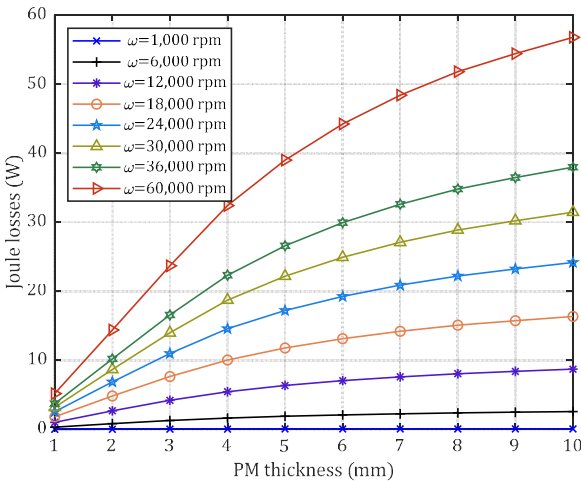


FIGURE 15 | Variation of losses with rotor PM thickness.

TABLE 5 | Parameters of EDBs with different numbers of coils.

Winding type	Multi-phase
Eccentricity	0.1 mm
Air-gap length (l_g)	1 mm
Outer diameter	50 mm
Axial length	100 mm
PM thickness (PM_{th})	5 mm
Back iron thickness ($iron_{th}$)	5 mm
Number of coils	1–19
PM pole-pair number	4

EDB, a maximum of 9 coils would be recommended, since a further increase in the number of coils, would result in increased complexity with comparatively smaller improvements in restoring force production.

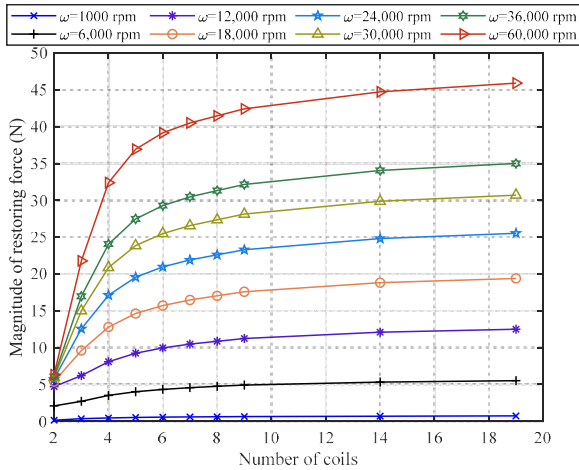


FIGURE 16 | Variation of the parallel forces with the number of coils.

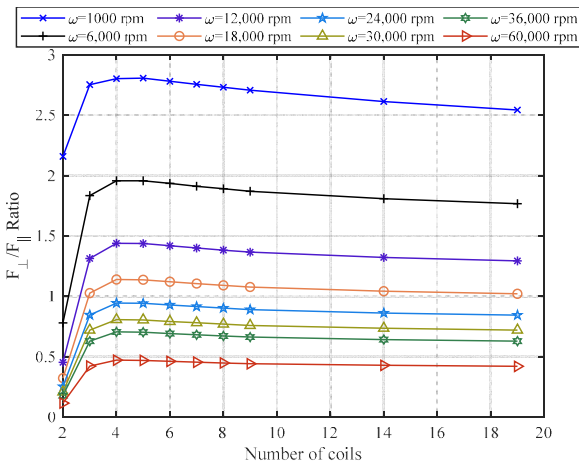


FIGURE 17 | Variation of the ratio of perpendicular force to parallel force with number of coils.

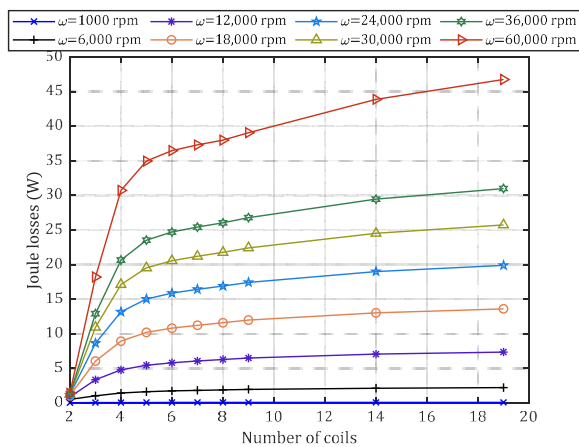


FIGURE 18 | Variation of losses with number of coils.

3.5 | Effect of Fill Factor

The previous analysis assumed ideal slot fill factor of 100%, which can only be achieved using solid conductors. However, exposing a solid conductor to a high frequency varying magnetic field, will result in significant eddy current losses, with or without eccentricity as well as increase the AC resistance of the winding. Therefore, multi-strand conductors, preferably Litz wires would be recommended, which will inevitably reduce the winding copper fill factor and increase the resistance of the coils. Therefore, understanding the effect of fill factor on the performance of the EDB is crucial.

Figure 19 shows the variation of the magnitude of the parallel restoring force with the fill factor at different speeds. It can be seen the fill factor has a significant effect on the magnitude of restoring force. Figure 20 shows the variation of the stability threshold speed of the EDB with the fill factor. Again, the effect of the fill factor is even more pronounced, particularly for values smaller than 0.5. However, it can also be noticed that for a fill factor larger than 0.5, the stability threshold speed is fairly

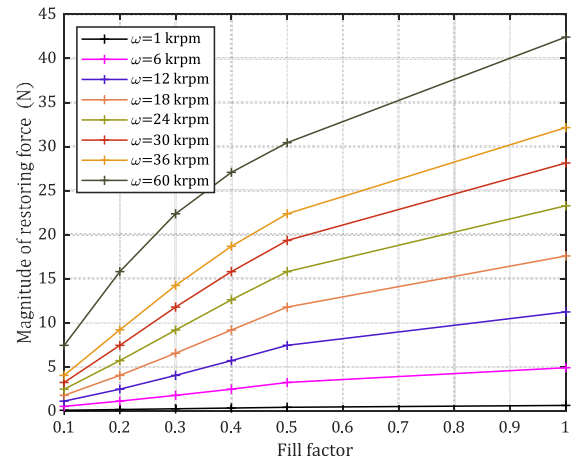


FIGURE 19 | Variation of restoring force (F_{\parallel}) with fill factor at different speeds.

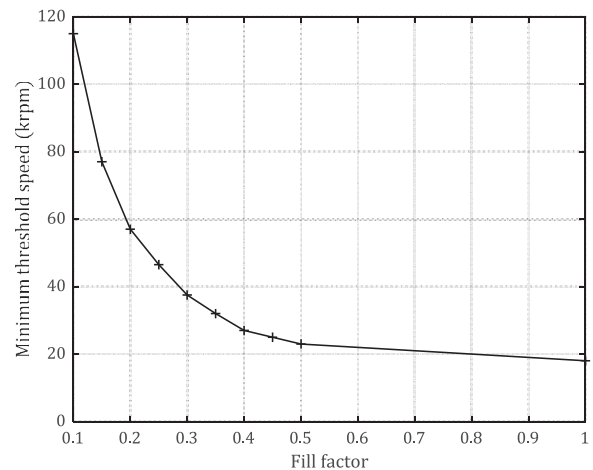


FIGURE 20 | Variation of the ratio of perpendicular force to parallel force with fill factor.

constant. Therefore, the manufacturing and the achievable winding fill factor must be considered at the early design stages of such EDBs.

4 | Experimental Validation

In order to test EDBs' performance under quasi-static conditions, a test rig is designed and built. The test rig enables the precise setting of eccentricity and the measurements of restoring force at both parallel and perpendicular axes. Figure 21 shows the schematic of the test rig. Two square-shaped aluminium panels connected by four aluminium bars form the main structure of the rig. The stationary part of the EDB, which

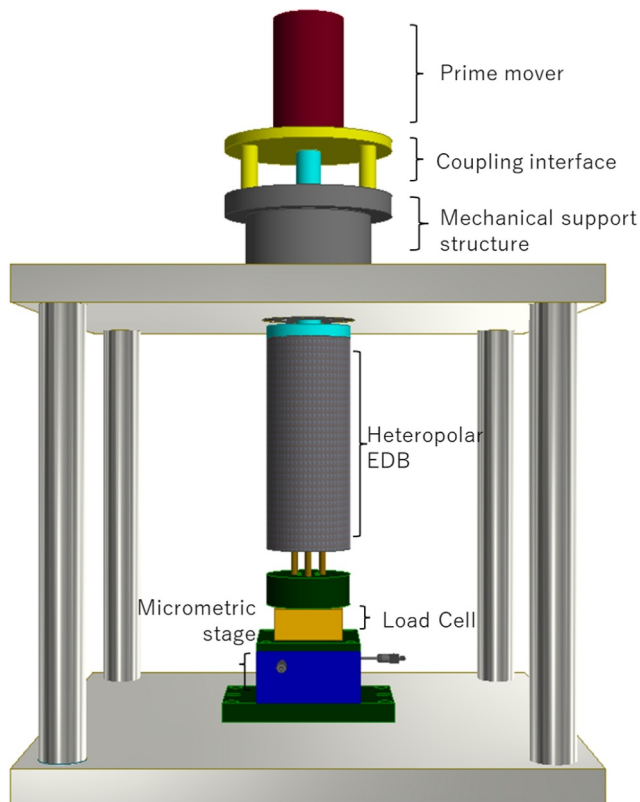


FIGURE 21 | Schematic of the experimental setup used to test the EDB.

carries the windings, is rigidly connected to the load cell via three stainless steel rods to allow for force transmission. On the other hand, EDB's external rotor is connected to an aluminium end cap which is rigidly coupled with the prime mover's shaft. A special mechanical structure supporting the weight of the rotor was made to ensure the true movement of the rotor.

The dimensions of the prototyped heteropolar multi-phase EDB are detailed in Table 5. However, its stator is equipped with nine equispaced short-circuited coils, with a span of 180° mechanical. The stator coils are mounted on a Tufnol cylinder, which is a nonmagnetic and nonconductive material.

After the stator position was calibrated with respect to the rotor position, the eccentricity is introduced using the micrometric positioning stage, and the restoring forces developed at different speeds are measured Figure 22.

Rotor eccentricity was varied between 0.1 and 0.5 mm. At each eccentricity value, forces in both parallel and perpendicular axes are measured at different rotational speeds. Because of safety and cost considerations, the purpose of the test rig is only to validate the predictions at a low-speed operation, where the EDB is unstable, and the force perpendicular to the eccentricity is significantly larger than the parallel components. Therefore, the accuracy in the measurement of the parallel component is limited. Figures 23 and 24 show the measured and predicted restoring forces in the parallel and perpendicular axes, respectively. A good correlation between the predicted and measured results is shown, particularly in the perpendicular direction where the measured forces are within the accurate range of the load cell.

5 | Conclusions

A winding configuration, which employs a set of short-circuited fully pitched individual coils, is presented. It has been shown that despite its simplicity, such winding configuration, exhibits similar performance, in terms of restoring force and stability speed threshold, to those recommended in the literature. Furthermore, the effects of the leading design parameters, such as PM thickness, pole-pair number, number of phases, etc., are investigated using 2D-FEA. It is shown that the winding fill

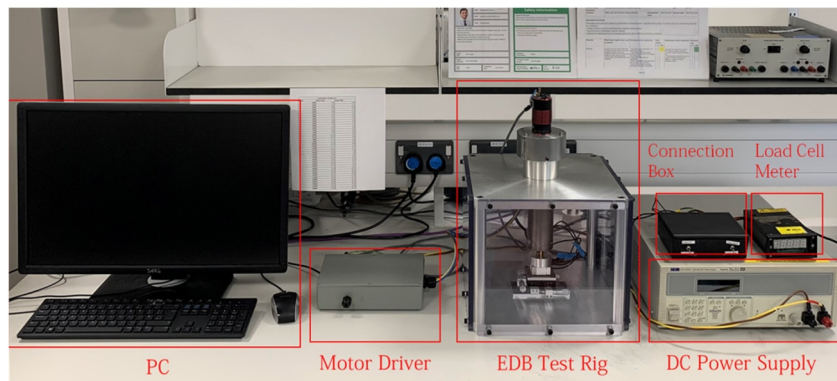


FIGURE 22 | Experiential set-up.

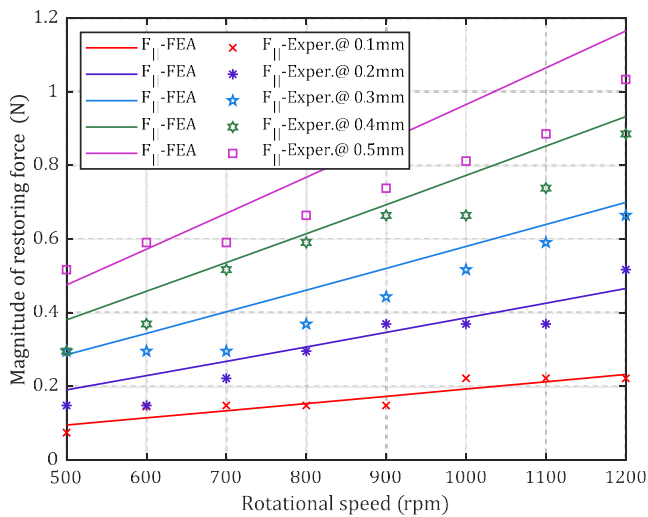


FIGURE 23 | Measured and predicted parallel forces with rotational speed at different values of eccentricity.

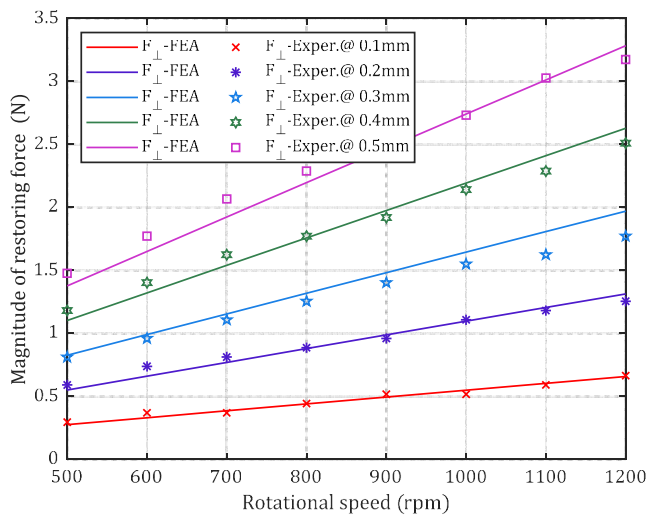


FIGURE 24 | Measured and predicted perpendicular forces with rotational speed at different values of eccentricity.

factor, in particular, can have significant effects and should be considered at the very early design stages.

A test rig is developed to test the performance of the prototype EDB under quasi-static conditions, at low speeds and varying eccentricities. Good agreement between measured and predicted results is noticed, particularly for the significantly larger perpendicular component.

Author Contributions

Abdoalateef Alzhrani: conceptualization, formal analysis, investigation, methodology, validation, writing – original draft, writing – review and editing. **Kais Atallah:** conceptualization, methodology, project administration, resources, supervision, writing – review and editing.

Acknowledgements

The work was undertaken at the University of Sheffield, UK. Furthermore, the authors would like to express their gratitude to JMAG International for providing the JMAG-Designer software licence, which was essential for the design and analysis of the EDBs.

Conflicts of Interest

The authors declare no conflicts of interest.

Data Availability Statement

The data that support the findings of this study are available from the corresponding author upon reasonable request.

References

1. D. K. Supreeth, S. I. Bekinal, and S. R. Chandranna, “An Overview on Electrodynamic Bearings,” *IEEE Access* 10 (2022): 57437–57451, <https://doi.org/10.1109/access.2022.3176632>.
2. P. K. Budig, “Magnetic Bearings and Some New Applications,” in *The XIX International Conference on Electrical Machines—ICEM 2010* (IEEE, 2010), 1–7.
3. A. V. Filatov and E. H. Maslen, “Passive Magnetic Bearing for Flywheel Energy Storage Systems,” *IEEE Transactions on Magnetics* 37, no. 6 (November 2001): 3913–3924, <https://doi.org/10.1109/20.966127>.
4. D. Dutta, P. Kumar Biswas, S. Debnath, and F. Ahmad, “Advancements and Challenges in Active Magnetic Bearings: A Comprehensive Review of Performance, Control and Future Prospects,” *IEEE Access* 13 (2025): 3051–3071, <https://doi.org/10.1109/access.2024.3523205>.
5. A. Kandil and Y. S. Hamed, “Tuned Positive Position Feedback Control of an Active Magnetic Bearings System WITH 16-Poles and Constant Stiffness,” *IEEE Access* 9 (2021): 73857–73872, <https://doi.org/10.1109/access.2021.3080457>.
6. J. Detoni, “Progress on Electrodynamic Passive Magnetic Bearings for Rotor Levitation,” *Proceedings of the Institution of Mechanical Engineers - Part C: Journal of Mechanical Engineering Science* 228, no. 10 (2014): 1829–1844, <https://doi.org/10.1177/0954406213511798>.
7. T. S. Slininger, et al., “An Overview on Passive Magnetics Bearings,” in *IEEE International Electric Machines & Drives Conference (IEMDC)* (IEEE, 2021).
8. K. Boden and J. K. Fremerey, “Industrial Realization of the ‘System KFA-Jülich’ Permanent Magnet Bearing Lines,” in *Proceedings of MAG 92* (SAGE, 1992), 43–61.
9. T. Wu and W. Zhang, “Review on Key Development of Magnetic Bearings,” *Machines* 13, no. 113 (2025): 113, <https://doi.org/10.3390/machines13020113>.
10. C. Murakami, “All-Passive-Type Rotary Magnetic Bearing System Based on Stability Principle of Sleeping Tops,” *JSME International Journal, Dynamics, Control, Robotics, Design and Manufacturing* 38, no. 3 (1995): 601–608, <https://doi.org/10.1299/jsmec1993.38.601>.
11. Y. Chen, W. Zhang, J. Z. Bird, S. Paul, and K. Zhang, “A 3-D Analytic Based Model of a Null-Flux Halbach Array Electrodynamic Suspension Device,” *IEEE Transactions on Magnetics* 51, no. 11 (2015): 1–5, <https://doi.org/10.1109/tmag.2015.2444331>.
12. R. Larsson, *Design and Control of Active Magnetic Bearing Systems for High Speed Rotation*. PhD thesis (Swiss Federal Institute of Technology, 1990).
13. Q. Cui, “Stabilization of Electrodynamic Bearings With Active Magnetic Dampers,” in *Doctor of Philosophy, Laboratory of Robotic Systems* (Swiss Federal Institute of Technology, 2016).

14. M. Siebert, et al., *A Passive Magnetic Bearing Flywheel* (36th Inter-society Energy Conversion Engineering Conference, 2001).
15. H. Bleuler, J. Sandtner, Y. Regamey, and F. Barrot, "Passive Magnetic Bearings for Flywheels," in *Solid Mechanics and Its Applications*, (Springer 2005).
16. N. Tanase and A. M. Morega, 'Passive Magnetic Bearings for Flywheel Energy Storage – Numerical Design' *International Conference on Applied and Theoretical Electricity* (ICATE, 2014).
17. S. Earnshaw, "On the Nature of the Molecular Forces Which Regulate the Constitution of the Luminiferous Ether' Transactions on the Cambridge," *Philosophical Society* 7 (1842): 97–112.
18. T. A. Lembke, "Design and Analysis of a Novel Low Loss Homopolar Electrodynamic Bearing," in *Doctor of Philosophy, Department of Electrical Engineering* (Royal Institute Of Technology, 2005).
19. T. A. Lembke, "Review of Electrodynamic Bearings," in *International Symposium on Magnetic Bearings* (Linz, 2014).
20. D. Rura, et al., "Design and Analysis of Homopolar Electrodynamic Bearing With Radial Magnets," in *International Conference on Electrical Machines* (IEEE, 2022).
21. A. Alzhrani and K. Atallah, "Novel Passive Electrodynamic Magnetic Bearings," in *2022 IEEE Energy Conversion Congress and Exposition (ECCE)* (IEEE, 2022), 1–7.
22. R. F. Post, "Passive Magnetic Bearing System," Patent US20120175985A1 (2012).
23. C. Dumont, V. Kluyskens, and B. Dehez, "Null-Flux Radial Electrodynamic Bearing," *IEEE Transactions on Magnetics* 50, no. 10 (2014): 1–12, <https://doi.org/10.1109/tmag.2014.2323292>.
24. C. Dumont, et al., "Performance of Yokeless Heteropolar Electrodynamic Bearings," *ACES Journal* 32, no. 8 (2017): 685–690, <https://doi.org/10.1016/j.matcom.2015.10.003>.